Power Electronic Systems
Laboratory

Proceedings of the 16th European Conference on Power Electronics and Applications (EPE 2014 - ECCE Europe), Lappeenranta, Finland, August 26-28, 2014

Analysis and Practical Relevance of CM/DM EMI Noise Separator Characteristics

S. Schroth,
F. Krismer,
J. W. Kolar,
H. Ertl

Eidgenössische Technische Hochschule Zürich
Swiss Federal Institute of Technology Zurich

Analysis and Practical Relevance of CM/DM EMI Noise Separator Characteristics

Sebastian Schroth[1], Florian Krismer[1], Johann W. Kolar[1], Hans Ertl[2]
[1]Power Electronic Systems Laboratory, ETH-Zurich, Switzerland
[2]Vienna University of Technology, Austria
Email: schroth@lem.ee.ethz.ch, krismer@lem.ee.ethz.ch,
kolar@lem.ee.ethz.ch, jertl@pop.tuwien.ac.at
URL: http://www.pes.ee.ethz.ch

Keywords

<<EMC/EMI>>, <<Noise>>.

Abstract

This Paper details two different contributions related to practical CM/DM EMI measurements. A first part investigates sources and implications of measurement errors that result for CM/DM separators in a practical measurement environment with a particular focus on the recently presented input impedance criterion for CM/DM separators. Furthermore, the realization of an active CM/DM separator, which features competitive separation capabilities ($DMTR/CMRR >$ 51 dB and $CMTR/DMRR > 47$ dB for frequencies up to 10 MHz), is presented.

Introduction

The practical applicability of different CM/DM separators, used to determine Common Mode (CM) and Differential Mode (DM) components of the conducted EMI noise generated by a switched mode power supply, is investigated. In this context, the PFC rectifier of the variable speed drive system depicted in **Fig. 1**, which features a maximum output power of 500 W, serves as a suitable platform for experimental verification. The single-phase PFC rectifier is needed to meet the mains current harmonic requirements, e.g. according to [1], and to achieve a high power factor (typically greater 0.9). The employed inverter facilitates speed control of an electric machine. The maximum allowable levels of conducted EMI noise in each mains phase are limited according to IEC 61000-6-3 [2] in the frequency range between 150 kHz and 30 MHz. Thus, in order to meet the specified requirements, an EMI filter, e.g. designed according to [3], is inserted between the mains connection and the power converter as shown in Fig. 1. The effectiveness of the EMI filter is verified with the measurement set-up depicted in **Fig. 2** [4], which employs Artificial Mains Networks (AMNs), depicted in **Fig. 3**, in each phase in order to achieve reproducible measurements, i.e. independent of the mains impedance. The AMN, in addition, separates the high frequency EMI noise from the mains frequency supply current and provides this high fre-

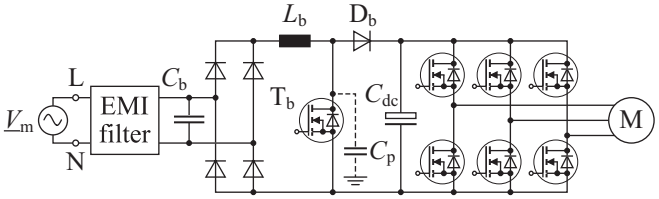

Figure 1: The considered power converter system: single-phase PFC rectifier and inverter power an electric machine. The system is designed for a nominal output power of 500 W and a 230 V / 50 Hz mains.

quency EMI noise to a 50 Ω receiver at its measurement port.

Initial measurements of conducted EMI noise often reveal insufficient filter attenuation, in particular at high frequencies above 1 MHz. In this context, the question arises how actual deficiencies of the EMI filter can be resolved in a systematic way. Since the EMI filter employs essentially different filter components to suppress Differential Mode (DM) and Common Mode (CM) EMI noise, a common approach for a diagnostic inspection is to separate the conducted EMI noise into Differential Mode (DM) and Common Mode (CM) noise. Direct measurement of DM and CM EMI noise is feasible with the measurement set-up depicted in **Fig. 4**, which employs a CM/DM separator and facilitates the measurements of the conducted DM and CM EMI noise without and with EMI filter.

With the results obtained from these measurements it is possible to trace reasons for insufficient filter attenuations, cf. [3].

A literature review reveals numerous different realizations of single-phase CM/DM separators, which can be categorized according to list below.

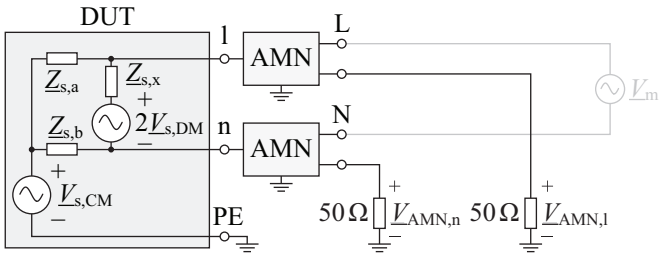

Figure 2: Measurement set-up used to determine the conducted EMI noise levels $V_{\mathrm{AMN,l}} = |\underline{V}_{\mathrm{AMN,l}}|$ and $V_{\mathrm{AMN,n}} = |\underline{V}_{\mathrm{AMN,n}}|$ (on the basis of [4]). The Device Under Test (DUT), modeled according to [16], denotes the source of conducted EMI. The AMNs separate the high frequency EMI noise from the mains frequency supply current and allow for reproducible measurements.

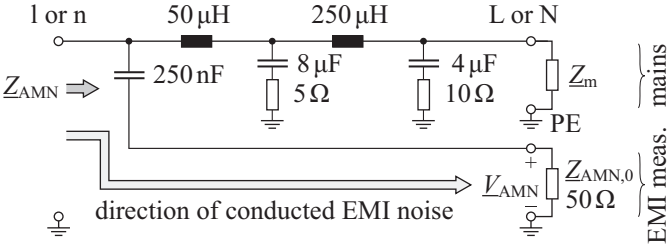

Figure 3: Schematic drawing of a commonly used AMN.

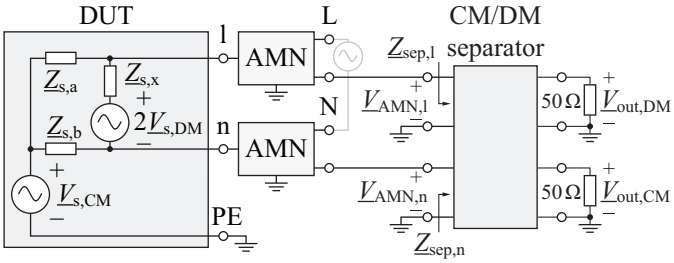

Figure 4: Measurement set-up employing a CM/DM separator to directly provide the DM and CM components of the conducted EMI noise to a test receiver.

1. *Passive separators* suppress either DM or CM component and preserve the remaining CM or DM component, respectively. Examples are CM/DM separators realized with resistor networks [7] and separators that employ broadband transformers [5–10].

2. *Active separators* employ operational amplifiers to determine DM and CM components [11, 12].

3. *Digital or software solutions*, e.g. with the use of digital oscilloscopes [13, 14].

4. *Direct measurement* of CM and DM components with current probes [15].

All CM/DM separators feature limited measurement accuracy, in particular due to limited CM and DM separation capabilities. In this context, the CM and DM transmission and rejection ratios (CMTR, DMTR, CMRR, and DMRR, cf. Section 1) are criteria used for evaluating CM/DM separators [10]. In addition to limited separation capability of the separator itself, however, also interactions at the interfaces between the AMNs' output ports and the separator's input ports in Fig. 4 may deteriorate the accuracy of the measured output voltages [16].

This Paper evaluates the practicability of different CM/DM separators and, first, reveals common properties of CM/DM separators in **Section 1**, i.e. input-side impedance characteristics

and CMTR, DMTR, CMRR, and DMRR values. Based on this summary the measurement errors that result in a practical measurement set-up are estimated in **Section 2**. The definitions given in Section 1 further facilitate the evaluation of a realized and improved version of an active CM/DM separator circuit, originally proposed in [11, 12], in **Section 3**, which uses operational amplifiers and features competitive noise separation capability with $DMTR/CMRR > 51\,\mathrm{dB}$ and $CMTR/DMRR > 47\,\mathrm{dB}$ for frequencies up to 10 MHz. Experimental results accompany the presented investigations.

1 Properties of single-phase CM/DM separators

Any single-phase CM/DM separator senses two input voltages at its input ports, e.g. $\underline{V}_{\mathrm{sep,l}}$ and $\underline{V}_{\mathrm{sep,n}}$ in **Fig. 5**, and processes the measured voltages in order to determine DM and CM components, which, in case of ideal separation, directly provides the values of the input-side DM and CM components,[1]

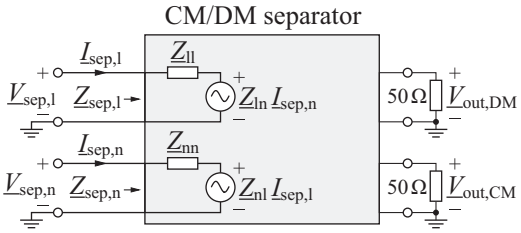

Figure 5: Characterization of the input ports of a CM/DM separator based on impedance matrix coefficients [16].

$$\underline{V}_{\mathrm{sep,DM}} = \frac{\underline{V}_{\mathrm{sep,l}} - \underline{V}_{\mathrm{sep,n}}}{2} \qquad (1)$$

$$\underline{V}_{\mathrm{sep,CM}} = \frac{\underline{V}_{\mathrm{sep,l}} + \underline{V}_{\mathrm{sep,n}}}{2}, \qquad (2)$$

at its output ports, i.e. $\underline{V}_{\mathrm{out,DM}} = \underline{V}_{\mathrm{sep,DM}}$ and $\underline{V}_{\mathrm{out,CM}} = \underline{V}_{\mathrm{sep,CM}}$.
In a practical realization the accuracy achievable for $\underline{V}_{\mathrm{out,DM}}$ and $\underline{V}_{\mathrm{out,CM}}$ is limited. This is partly due to to an unsuitable input impedance matrix of the CM/DM separator,

$$\underline{\mathbf{Z}}_{\mathrm{sep}} = \begin{pmatrix} \underline{Z}_{\mathrm{ll}} & \underline{Z}_{\mathrm{ln}} \\ \underline{Z}_{\mathrm{nl}} & \underline{Z}_{\mathrm{nn}} \end{pmatrix} \neq \underline{\mathbf{Z}}_{\mathrm{sep,ideal}} = \begin{pmatrix} 50\,\Omega & 0 \\ 0 & 50\,\Omega \end{pmatrix}, \qquad (3)$$

cf. Fig. 5, which introduces errors to $\underline{V}_{\mathrm{sep,l}}$ and $\underline{V}_{\mathrm{sep,n}}$ [16]. Further measurement errors arise from inaccurate processing of the measured voltages, commonly accounted for with gain errors [Differential Mode Transmission Ratio (DMTR) and / or Common Mode Transmission Ratio (CMTR) different to 0 dB] and cross coupling [Common Mode Rejection Ratio (CMRR) and / or Differential Mode Rejection Ratio (DMRR) greater than zero, i.e. greater than $-\infty\,\mathrm{dB}$]. DMTR, CMTR, CMRR, and DMRR are defined according to [10]:

$$DMTR = \left|\frac{\underline{V}_{\mathrm{out,DM}}}{\underline{V}_{\mathrm{sep,DM}}}\right|,\ CMTR = \left|\frac{\underline{V}_{\mathrm{out,CM}}}{\underline{V}_{\mathrm{sep,CM}}}\right|,\ CMRR = \left|\frac{\underline{V}_{\mathrm{out,DM}}}{\underline{V}_{\mathrm{sep,CM}}}\right|,\ DMRR = \left|\frac{\underline{V}_{\mathrm{out,CM}}}{\underline{V}_{\mathrm{sep,DM}}}\right|. \qquad (4)$$

These four factors allow for the estimation of the maximum output voltages including gain errors and cross coupling, which is detailed in Section 2.3.2.

2 Measurement errors in a practical set-up

2.1 Impact of $\underline{\mathbf{Z}}_{\mathrm{sep}}$ on the measurement result, simplified analysis

Fig. 4 depicts the basic measurement set-up used to determine DM and CM EMI noise. A more practical set-up, however, employs precision attenuators between the AMNs and the noise

[1] N.B.: In this document, variables with underlined capital letters denote phasors; $\underline{V}_{\mathrm{out,DM}} = V_{\mathrm{out,DM}}\,\mathrm{e}^{\mathrm{j}\varphi_{\mathrm{out,DM}}}$, for example, denotes the phasor of the DM output voltage with a RMS value of $V_{\mathrm{out,DM}}$ and a relative phase angle equal to $\varphi_{\mathrm{out,DM}}$, cf. [3].

separator, according to **Fig. 6**, to terminate the AMNs with almost constant load impedances, $\underline{Z}_{\mathrm{att,in,l}}$ and $\underline{Z}_{\mathrm{att,in,n}}$, close to 50 Ω. The T-type attenuator network depicted in **Fig. 7**, for example, features an attenuation of 20 dB and provides an input impedance between 49 Ω and 51 Ω, depending on whether the attenuator's output is terminated with a short-circuit or an open-circuit, respectively.[2] The shown 20 dB-attenuator, in addition, provides a well-defined voltage source at its output side, e.g. the attenuator connected to the L-phase provides an open-circuit voltage of $\underline{V}_{\mathrm{AMN,l}}/5.05$ with an inner impedance of $\underline{Z}_{\mathrm{att,out,l}} \approx 50\,\Omega$. Thus, with the separator model depicted in Fig. 5, the circuit diagram of **Fig. 8** can be established. In a first step, the circuit of Fig. 8 facilitates the calculation of the separator's input voltages, $\underline{V}_{\mathrm{sep,l}}$ and $\underline{V}_{\mathrm{sep,n}}$. This, in a second step, enables the calculation of the DM and CM voltages, $\underline{V}_{\mathrm{out,DM}}$ and $\underline{V}_{\mathrm{out,CM}}$, that are applied to the test receiver, which, in a third step, allows for the calculation of the implications of $\underline{\mathbf{Z}}_{\mathrm{sep}} \neq \underline{\mathbf{Z}}_{\mathrm{sep,ideal}}$, cf. (3), on the measurement result.

The separator's input voltages can be calculated by solving the corresponding equation system,

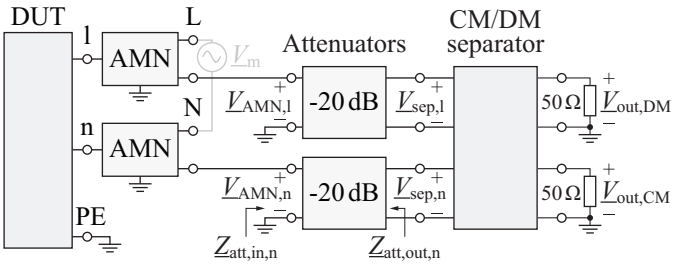

Figure 6: EMI measurement set-up including precision attenuators, here with an attenuation of 20 dB, between the AMNs and the CM/DM separator.

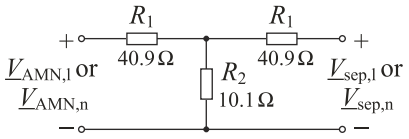

Figure 7: Resistances used in a 50 Ω T-type attenuator network that provides an attenuation of 20 dB.

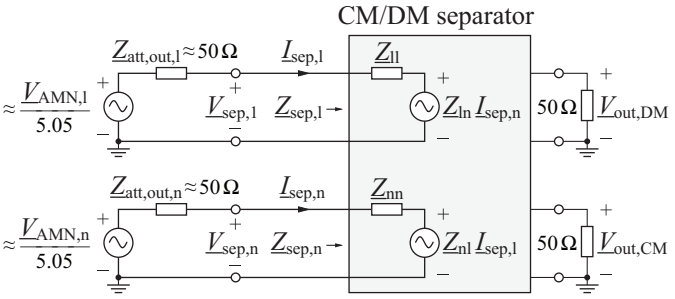

Figure 8: Simplified model used to estimate the errors in the measured DM and CM components that arise from a non-ideal input impedance matrix of the CM/DM separator, cf. (7).

$$\frac{\underline{V}_{\mathrm{AMN,l}}}{5.05} = (\underline{Z}_{\mathrm{att,out,l}} + \underline{Z}_{\mathrm{ll}})\underline{I}_{\mathrm{sep,l}} + \underline{Z}_{\mathrm{ln}}\underline{I}_{\mathrm{sep,n}}, \quad \frac{\underline{V}_{\mathrm{AMN,n}}}{5.05} = (\underline{Z}_{\mathrm{att,out,n}} + \underline{Z}_{\mathrm{nn}})\underline{I}_{\mathrm{sep,n}} + \underline{Z}_{\mathrm{nl}}\underline{I}_{\mathrm{sep,l}},$$

with respect to $\underline{I}_{\mathrm{sep,l}}$ and $\underline{I}_{\mathrm{sep,n}}$ and inserting the solutions to

$$\underline{V}_{\mathrm{sep,l}} = \underline{Z}_{\mathrm{ll}}\underline{I}_{\mathrm{sep,l}} + \underline{Z}_{\mathrm{ln}}\underline{I}_{\mathrm{sep,n}}, \qquad \underline{V}_{\mathrm{sep,n}} = \underline{Z}_{\mathrm{nn}}\underline{I}_{\mathrm{sep,n}} + \underline{Z}_{\mathrm{nl}}\underline{I}_{\mathrm{sep,l}},$$

which gives

$$\underline{V}_{\mathrm{sep,l}} = \frac{\underline{V}_{\mathrm{AMN,n}}\underline{Z}_{\mathrm{ln}}\underline{Z}_{\mathrm{att,out,l}} + \underline{V}_{\mathrm{AMN,l}}\left[\underline{Z}_{\mathrm{ll}}\left(\underline{Z}_{\mathrm{nn}} + \underline{Z}_{\mathrm{att,out,l}}\right) - \underline{Z}_{\mathrm{ln}}\underline{Z}_{\mathrm{nl}}\right]}{5.05\left[\left(\underline{Z}_{\mathrm{ll}} + \underline{Z}_{\mathrm{att,out,l}}\right)\left(\underline{Z}_{\mathrm{nn}} + \underline{Z}_{\mathrm{att,out,n}}\right) - \underline{Z}_{\mathrm{ln}}\underline{Z}_{\mathrm{nl}}\right]},$$

$$\underline{V}_{\mathrm{sep,n}} = \frac{\underline{V}_{\mathrm{AMN,l}}\underline{Z}_{\mathrm{nl}}\underline{Z}_{\mathrm{att,out,n}} + \underline{V}_{\mathrm{AMN,n}}\left[\underline{Z}_{\mathrm{nn}}\left(\underline{Z}_{\mathrm{ll}} + \underline{Z}_{\mathrm{att,out,n}}\right) - \underline{Z}_{\mathrm{ln}}\underline{Z}_{\mathrm{nl}}\right]}{5.05\left[\left(\underline{Z}_{\mathrm{ll}} + \underline{Z}_{\mathrm{att,out,l}}\right)\left(\underline{Z}_{\mathrm{nn}} + \underline{Z}_{\mathrm{att,out,n}}\right) - \underline{Z}_{\mathrm{ln}}\underline{Z}_{\mathrm{nl}}\right]}.$$

In these two equations, the AMN output voltages $\underline{V}_{\mathrm{AMN,n}}$ and $\underline{V}_{\mathrm{AMN,l}}$ are advantageously replaced by the corresponding CM and DM components,

$$\underline{V}_{\mathrm{AMN,l}} = \underline{V}_{\mathrm{AMN,CM}} + \underline{V}_{\mathrm{AMN,DM}}, \qquad \underline{V}_{\mathrm{AMN,n}} = \underline{V}_{\mathrm{AMN,CM}} - \underline{V}_{\mathrm{AMN,DM}}. \tag{5}$$

[2] Still, a sufficiently high voltage level is available at the input of the test receiver, since modern test receivers feature useful operation for input voltages as low as ≈ 15 dBμV, which is considerably less than the allowable limits of conducted EMI noise defined in [2] minus 20 dB.

The expressions resulting for $\underline{V}_{\mathrm{sep,l}}$ and $\underline{V}_{\mathrm{sep,n}}$ are processed according to (1) in order to determine the CM and DM components of the separator's input voltages, $\underline{V}_{\mathrm{sep,DM}}$ and $\underline{V}_{\mathrm{sep,CM}}$. Finally, the expressions obtained for $\underline{V}_{\mathrm{sep,DM}}$ and $\underline{V}_{\mathrm{sep,CM}}$ are processed using the definitions of (4) in order to calculate the maximum values expected at the separator's output ports, $\max\left(V_{\mathrm{out,DM}}\right)$ and $\max\left(V_{\mathrm{out,CM}}\right)$, cf. (11). Even though this calculation is straight-forward, large expressions result for $\max\left(V_{\mathrm{out,DM}}\right)$ and $\max\left(V_{\mathrm{out,CM}}\right)$. In a first approach, the assumptions listed below are made to allow for a simplified calculation of the measurement error expected for $\underline{\mathbf{Z}}_{\mathrm{sep}} \neq \underline{\mathbf{Z}}_{\mathrm{sep,ideal}}$ (more in-depth investigations are detailed in the subsequent Sections 2.2 and 2.3).

- Ideal transfer ratios: $DMTR = CMTR = 0\,\mathrm{dB}$.
- No cross couplings: $DMRR \to -\infty\,\mathrm{dB}$ and $CMRR \to -\infty\,\mathrm{dB}$.
- Set-up is ideally symmetric: $\underline{Z}_{\mathrm{att,out,l}} = \underline{Z}_{\mathrm{att,out,n}}$, $\underline{Z}_{\mathrm{ll}} = \underline{Z}_{\mathrm{nn}}$, and $\underline{Z}_{\mathrm{ln}} = \underline{Z}_{\mathrm{nl}}$.

With these assumptions the magnitudes of $\underline{V}_{\mathrm{out,DM}}$ and $\underline{V}_{\mathrm{out,CM}}$ can be calculated:

$$V_{\mathrm{out,DM}} = \frac{V_{\mathrm{AMN,DM}}}{5.05}\left|\frac{\underline{Z}_{\mathrm{ll}} - \underline{Z}_{\mathrm{ln}}}{\underline{Z}_{\mathrm{att,out,l}} + \underline{Z}_{\mathrm{ll}} - \underline{Z}_{\mathrm{ln}}}\right|, \quad V_{\mathrm{out,CM}} = \frac{V_{\mathrm{AMN,CM}}}{5.05}\left|\frac{\underline{Z}_{\mathrm{ll}} + \underline{Z}_{\mathrm{ln}}}{\underline{Z}_{\mathrm{att,out,l}} + \underline{Z}_{\mathrm{ll}} + \underline{Z}_{\mathrm{ln}}}\right|. \tag{6}$$

It is important to note that the CM and DM components are decoupled in (6) (and, thus, in the set-up depicted in Fig. 6), i.e. $V_{\mathrm{out,DM}}$ does not depend on $V_{\mathrm{AMN,CM}}$ and $V_{\mathrm{out,CM}}$ does not depend on $V_{\mathrm{AMN,DM}}$. Therefore, only DM and CM gain errors,

$$e_{\mathrm{DM}} = \frac{V_{\mathrm{out,DM}}|_{\underline{\mathbf{Z}}_{\mathrm{sep}} \neq \underline{\mathbf{Z}}_{\mathrm{sep,ideal}}}}{V_{\mathrm{out,DM}}|_{\underline{\mathbf{Z}}_{\mathrm{sep}} = \underline{\mathbf{Z}}_{\mathrm{sep,ideal}}}}, \qquad e_{\mathrm{CM}} = \frac{V_{\mathrm{out,CM}}|_{\underline{\mathbf{Z}}_{\mathrm{sep}} \neq \underline{\mathbf{Z}}_{\mathrm{sep,ideal}}}}{V_{\mathrm{out,CM}}|_{\underline{\mathbf{Z}}_{\mathrm{sep}} = \underline{\mathbf{Z}}_{\mathrm{sep,ideal}}}}, \tag{7}$$

are to be expected for a separator with a non-ideal input impedance matrix if the measurement set-up shown in Fig. 6 is employed and if the above listed assumptions are met. With (6) the DM and CM gain errors are:

$$e_{\mathrm{DM}} = \left|\frac{\underline{Z}_{\mathrm{ll}} - \underline{Z}_{\mathrm{ln}}}{\underline{Z}_{\mathrm{att,out,l}} + \underline{Z}_{\mathrm{ll}} - \underline{Z}_{\mathrm{ln}}}\,\frac{\underline{Z}_0 + \underline{Z}_{\mathrm{att,out,l}}}{\underline{Z}_0}\right|, \; e_{\mathrm{CM}} = \left|\frac{\underline{Z}_{\mathrm{ll}} + \underline{Z}_{\mathrm{ln}}}{\underline{Z}_{\mathrm{att,out,l}} + \underline{Z}_{\mathrm{ll}} + \underline{Z}_{\mathrm{ln}}}\,\frac{\underline{Z}_0 + \underline{Z}_{\mathrm{att,out,l}}}{\underline{Z}_0}\right|. \tag{8}$$

A prominent CM/DM separator which does not fulfill the input impedance criteria defined with (3) is the CM/DM separator proposed by C. Paul in [5]. The input impedance matrix of this separator is:

$$\underline{\mathbf{Z}}_{\mathrm{sep,Paul}} = \begin{pmatrix} 50.6\,\Omega & \pm 31.4\,\Omega \\ \pm 31.4\,\Omega & 50.6\,\Omega \end{pmatrix}. \tag{9}$$

The $\pm$-sign denotes whether the circuit separates DM or CM, i.e. the sign is positive for DM separation and negative for CM separation. In combination with (8), same error factors result for DM and CM separation, $\underline{e}_{\mathrm{DM}} = \underline{e}_{\mathrm{CM}} = 0.555$, which corresponds to a gain error of $-5.1\,\mathrm{dB}$ compared to a DM/CM separator that facilitates an ideal input impedance matrix.

2.2 Impact of $\underline{\mathbf{Z}}_{\mathrm{sep}}$ on the measurement result, detailed analysis

According to the results given in the above Section 2.1 any symmetric input matrix impedance of a CM/DM separator is expected to not cause CM/DM cross coupling if the measurement set-up is completely symmetric, too. A real measurement set-up, however, may not be fully symmetric. Still, the resulting measurement error can be calculated for a more realistic measurement environment, too, using the more complete model depicted in **Fig. 9**. This includes a carefully

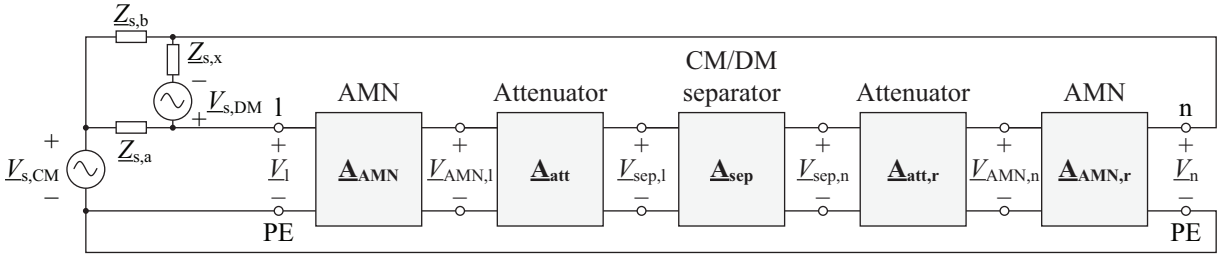

Figure 9: Detailed model used to verify e_{DM} and e_{CM} obtained for the simplified model and with the EMI noise source model from Fig. 2, cf. (8); AMNs, precision attenuators, and CM/DM separator are preferably modeled with cascade matrices; $\underline{\mathbf{A}}_{\mathrm{att,r}}$ and $\underline{\mathbf{A}}_{\mathrm{AMN,r}}$ are the reverse of $\underline{\mathbf{A}}_{\mathrm{att}}$ and $\underline{\mathbf{A}}_{\mathrm{AMN}}$.

Designator	*Value*	*Description*
f_{s}	130 kHz	Switching frequency
L_{b}	465 µH	Inductance of the boost converter
C_{b}	470 nF	Input capacitance of the boost converter
C_{p}	15 pF	Parasitic capacitance between earth and the drain of the MOSFET

Table I: Design parameters and component values of the investigated PFC rectifier.

modeled EMI noise source, the CM/DM separator model of Fig. 5, and AMN and attenuator networks (N.B.: $\underline{\mathbf{A}}_{\mathrm{att,r}}$ and $\underline{\mathbf{A}}_{\mathrm{AMN,r}}$ denote the reverse of $\underline{\mathbf{A}}_{\mathrm{att}}$ and $\underline{\mathbf{A}}_{\mathrm{AMN}}$, respectively).
In the course of a modeled example, the PFC rectifier circuit of Fig. 1 without EMI filter serves as a basis for configuring the EMI noise source (from [3, 16]):[3]

$$\underline{V}_{\mathrm{s}}(nf_{\mathrm{s}}) = \frac{1}{n}\sqrt{\frac{4}{\pi}V_{\mathrm{m,pk}}V_0 - V_{\mathrm{m,pk}}^2}\ \forall\ n \in \mathbb{N}, \quad \underline{V}_{\mathrm{s,DM}}(nf_{\mathrm{s}}) = \frac{\underline{V}_{\mathrm{s}}(nf_{\mathrm{s}})}{2} \cdot \frac{1}{1-(2\pi nf_{\mathrm{s}})^2 L_{\mathrm{b}}C_{\mathrm{b}}},$$

$$\underline{V}_{\mathrm{s,CM}} = \underline{V}_{\mathrm{s}}\,\mathrm{e}^{\mathrm{j}\pi}, \qquad \underline{Z}_{\mathrm{s,x}}(nf_{\mathrm{s}}) = \frac{\mathrm{j}2\pi nf_{\mathrm{s}}L_{\mathrm{b}}}{1-(2\pi nf_{\mathrm{s}})^2 L_{\mathrm{b}}C_{\mathrm{b}}},$$

$$\underline{Z}_{\mathrm{s,a}}(nf_{\mathrm{s}}) \to \infty, \qquad \underline{Z}_{\mathrm{s,b}}(nf_{\mathrm{s}}) = \frac{1}{2\pi nf_{\mathrm{s}}C_{\mathrm{p}}}.$$

Figures 10(a) and **(b)** depict the RMS values of the DM and CM output voltages calculated for this PFC rectifier, using the network of Fig. 9 with 20 dB precision attenuators and CM/DM separators with different input impedance matrices. The calculated results are in good agreement with (8): the separators with $\underline{\mathbf{Z}}_{\mathrm{sep}} = \underline{\mathbf{Z}}_{\mathrm{sep,ideal}}$ and $\underline{\mathbf{Z}}_{\mathrm{sep}} = \underline{\mathbf{Z}}_{\mathrm{sep,Paul}}$ return the same CM and DM components except for a gain error of −5.1 dB introduced by the circuit of [5].

2.3 Implications of limited accuracies on measurement errors

The results presented in the previous Section 2.2 consider AMNs and precision attenuators with ideal component values and CM/DM separators featuring ideal separation, i.e. $DMTR = CMTR = 0\,\mathrm{dB}$, $DMRR \to -\infty\,\mathrm{dB}$, and $CMRR \to -\infty\,\mathrm{dB}$. Precision attenuators, realized with low-tolerance components, are readily available. Commercially available realizations of AMNs, however, may be subject to fairly high input impedance tolerances [4]. The maximum

[3]The presented calculation considers the PFC rectifier without EMI filter in order to investigate the performance of CM/DM separators in case of an asymmetric DUT, i.e. for $\underline{Z}_{\mathrm{s,a}}$ being considerably different to $\underline{Z}_{\mathrm{s,b}}$ in Fig. 9. The results presented in Fig. 10 are calculated for ideal boost inductance and input capacitance in order to emphasize on the measurement error that results for a non-ideal input impedance matrix of the CM/DM separator. EMI filter and parasitic effects, including non-ideal frequency responses of L_{b} and C_{b}, are considered in the measurement results presented in Section 2.4 and Fig. 11.

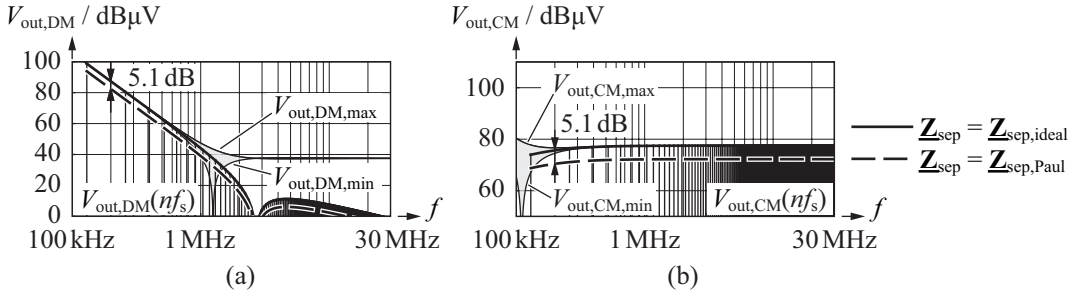

Figure 10: DM and CM components estimated for two different types of CM/DM separators, i.e. a separator with an ideal input impedance matrix, $\underline{\mathbf{Z}}_{\text{sep,ideal}}$, and the separator of [5] with $\underline{\mathbf{Z}}_{\text{sep,Paul}} \neq \underline{\mathbf{Z}}_{\text{sep,ideal}}$. The corresponding calculation is based on the network of Fig. 9, which has been parameterized according to Section 2.2 and considers a PFC rectifier without EMI filter to include the implications of asymmetric EMI noise source impedances on the calculated DM and CM components. The depicted shaded areas denote measurement uncertainties that result for $DMRR = -30\,\text{dB}$, $CMRR = -40\,\text{dB}$, and $DMTR = CMTR = 0\,\text{dB}$, cf. Section 2.3.2.

measurement errors expected for standard AMN realizations is detailed in Section 2.3.1. The measurement errors introduced by reason of limited CMRR- and DMRR-values of CM/DM separators are investigated in Section 2.3.2.

2.3.1 Tolerances specified for the AMN

According to [4], the allowable tolerances of magnitude and phase shift of the AMN's input impedance, $\underline{Z}_{\text{AMN}}$, are $\pm 20\%$ and $\pm 15°$, respectively. Thus, if only a DM or a CM component is applied to the inputs of the two AMNs, both, CM and DM, components result at the AMNs' outputs. A simplified calculation of the attenuation of the corresponding cross coupling reveals

$$Att_{\text{AMN,CM}\leftrightarrow\text{DM}} = \frac{\underline{Z}_{\text{AMN,0,l}} + \underline{Z}_{\text{AMN,0,n}}}{\underline{Z}_{\text{AMN,0,l}} - \underline{Z}_{\text{AMN,0,n}}}, \tag{10}$$

which, by reason of the high tolerance values, gives an unacceptably low minimum cross coupling attenuation of 9.5 dB.[4] Therefore, in this work, two identical AMN networks, using high precision components, have been realized for obtaining the presented experimental results.

2.3.2 CM/DM separators with limited values of CMRR and DMRR

Limited values of DMTR, CMTR, CMRR, and DMRR lead to an uncertainty of the measured DM and CM output voltages. Based on the corresponding definitions (4) it is straightforward to derive the respective limits for $V_{\text{out,DM}}$ and $V_{\text{out,CM}}$,

$$V_{\text{out,DM,min}} \leq V_{\text{out,DM}} \leq V_{\text{out,DM,max}}, \qquad V_{\text{out,CM,min}} \leq V_{\text{out,CM}} \leq V_{\text{out,CM,max}}. \tag{11}$$

The results for $V_{\text{out,DM,min}}$ and $V_{\text{out,DM,max}}$, for example, are:

$$\begin{aligned} V_{\text{out,DM,min}} &= |DMTR\; V_{\text{sep,DM}} - CMRR\; V_{\text{sep,CM}}|\,, \\ V_{\text{out,DM,max}} &= DMTR\; V_{\text{sep,DM}} + CMRR\; V_{\text{sep,CM}}. \end{aligned} \tag{12}$$

The shaded areas depicted in Fig. 10, plotted for $DMRR = -30\,\text{dB}$, $CMRR = -40\,\text{dB}$, and $DMTR = CMTR = 0\,\text{dB}$, denote points where the inequalities (11) hold true. In this Figure, the value of $V_{\text{out,DM}}$ becomes increasingly inaccurate for increasing frequencies and $f > 1\,\text{MHz}$, due to $V_{\text{sep,DM}}(f) < V_{\text{sep,CM}}(f)CMRR/DMTR$, cf. (12) [$V_{\text{sep,DM}}(f) = V_{\text{out,DM}}(f)$ and $V_{\text{sep,CM}}(f) = V_{\text{out,CM}}(f)$ would apply for an ideal separator]. Similarly, $V_{\text{out,CM}}$ becomes increasingly inaccurate for decreasing frequencies and $f < 200\,\text{kHz}$, due to $V_{\text{sep,CM}}(f) < V_{\text{sep,DM}}(f)DMRR/CMTR$.

[4] In the considered frequency range, $150\,\text{kHz} \leq f \leq 30\,\text{MHz}$, the above given tolerances are considered to approximately apply to the termination resistance connected to the measurement port of the AMN, $\underline{Z}_{\text{AMN,0}}$, since the AMN effectively redirects high frequency currents to the measurement port, cf. Fig. 3.

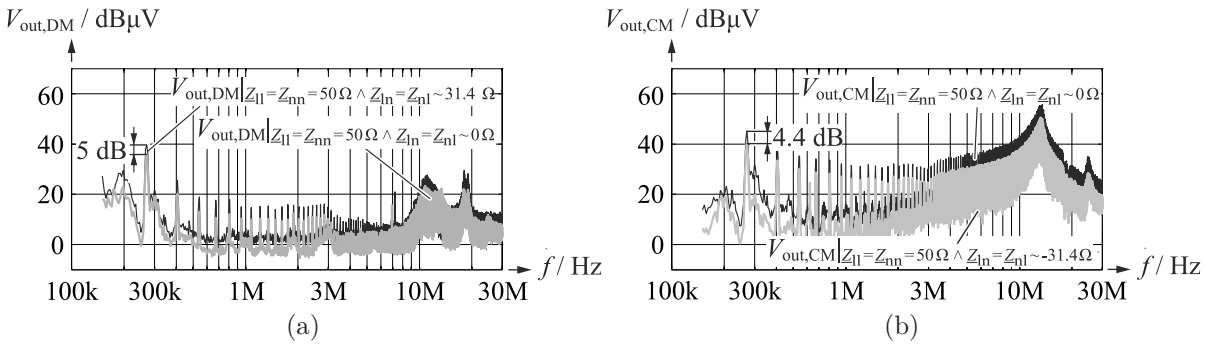

Figure 11: DM and CM components measured with two different types of CM/DM separators, i.e. a separator with an ideal input impedance matrix, $\underline{\mathbf{Z}}_{\mathrm{sep,ideal}}$, and the separator of [5] with $\underline{\mathbf{Z}}_{\mathrm{sep,Paul}} \neq \underline{\mathbf{Z}}_{\mathrm{sep,ideal}}$, and with 20 dB precision attenuators. Thus, 20 dB need to be added to the depicted values in order to obtain the actual CM and DM components of the generated EMI noise. N.B.: a gain of 6dB is inherent to the CM/DM separator of [5] and has been removed by means of initial calibration.

2.4 Comparison to measurement results

Figures 11(a) and **(b)** depict measured DM and CM components, which have been obtained for the considered PFC rectifier with EMI filters in order to avoid excessive high frequency load of the AMNs. The separator proposed by C. Paul [5] again provides output voltages that are approximately 5 dB below the output voltage measured with the separator proposed by S. Wang in [10], which features an input impedance matrix close to $\underline{\mathbf{Z}}_{\mathrm{sep,ideal}}$. The measurement, however, also includes additional errors in the higher frequency range, e.g. due to limited ratios of $DMTR/CMRR$ and $CMTR/DMRR$. Still, the difference of approximately 5 dB is clearly apparent for DM and CM components.

3 Performance achieved with an active CM/DM separator

A successful realization of a passive CM/DM separator includes careful optimization of broadband transformers and PCB layout in order to achieve acceptable separation capabilities in the required wide frequency range between 150 kHz and 30 MHz. The CM/DM separator, however, is subject to small signal excitations, i.e. the AMNs keep the supply currents away from it, a passive CM/DM separator can be directly replaced by an active realization, which allows for a straightforward implementation with relatively low effort, i.e. there is no need for cumbersome fine-tuning of the circuit.

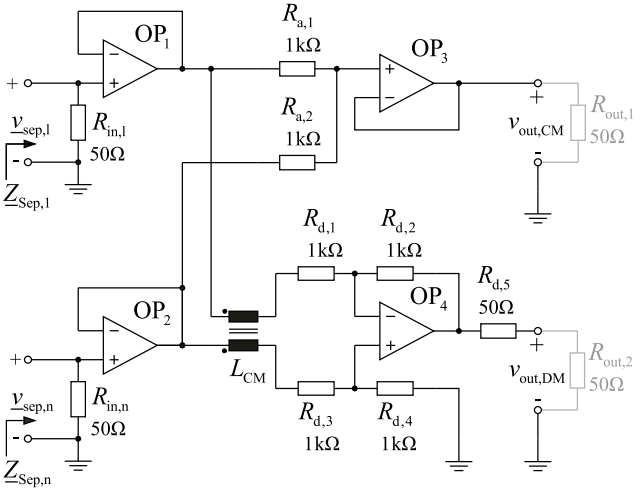

Figure 12: Schematic drawing of the presented active CM/DM separator.

Fig. 12 depicts the circuit of the considered active CM/DM separator, **Fig. 13** depicts a picture of the realized device. It employs four operational amplifiers: OP_1 and OP_2 realize an ideal input impedance matrix [together with $R_{\mathrm{in,l}}$ and $R_{\mathrm{in,n}}$, cf. (3)], and OP_3 and OP_4 determine the CM and DM voltages, respectively. Adequate operational amplifiers (in the presented circuit four AD8051 are used) and close-tolerance resistors need to be employed in order to achieve high CM/DM separation capability.

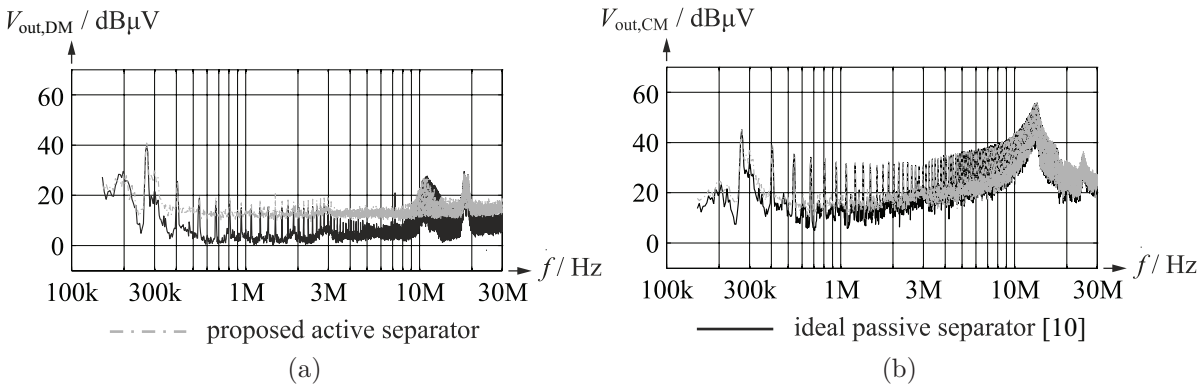

Figure 15: Illustrative comparison of the DM and CM components measured with the active and passive CM/DM separators (active separator: gray curve, passive separator: black curve) and with 20 dB precision attenuators. For the depicted results the passive CM/DM separator of [10] is selected, due to its ideal input impedance matrix.

The circuit, furthermore, includes a CM-choke, L_{CM}, to increase the $CMRR$ of the CM/DM separator. The resistor $R_{\mathrm{d},5}$, connected in series to the output of OP_4, is used to realize $DMTR = 0\,\mathrm{dB}$. Due to zero inner impedance of the CM output port, a short cable between the CM output port and the EMI test receiver is recommended in order to avoid measurement errors due to reflections.
According to **Fig. 14** the considered separator circuit features competitive values of $DMTR/CMRR$ and $CMTR/DMRR$ with $DMTR/CMRR > 51\,\mathrm{dB}$ and $CMTR/DMRR > 47\,\mathrm{dB}$ for frequencies up to 10 MHz. **Fig. 15** depicts the DM and CM EMI spectra measured with the passive separator of [10] and the proposed active separator. A visual inspection of these measurement results reveals only minor differences, e.g. the active separator generates a noise floor that is approximately 10 dB greater than that of the passive separator.

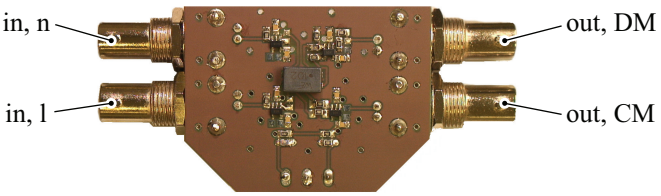

Figure 13: Picture of the active CM/DM separator revealing the low complexity of this circuit. The separator is powered from a 9 V-battery (connector at the bottom side).

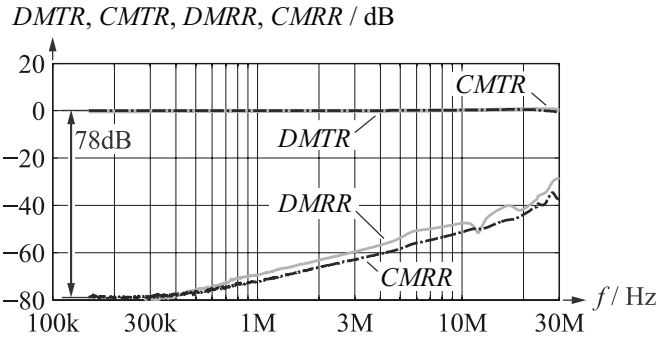

Figure 14: Measured values of DMTR, CMTR, DMRR, and CMRR of the considered active CM/DM separator depicted in Fig. 12. This separator features $DMTR/CMRR > 51\,\mathrm{dB}$ and $CMTR/DMRR > 47\,\mathrm{dB}$ for frequencies up to 10 MHz.

4 Discussion

The below list briefly summarizes the findings of this paper.

- In case of a non-ideal or an unknown input impedance matrix of the employed CM/DM separator it is advisable to consider the measurement set-up with precision attenuators depicted in Fig. 6 and to remove gain errors by means of an initial calibration (Sections 2.1 and 2.2). The precision attenuators may be omitted in case of a CM/DM separator with an ideal input impedance matrix; still, initial calibration is highly recommended.

- AMNs realized with close-tolerance components need to be employed, since the output impedances of commercially available AMNs may be subject to rather high tolerances,

which considerably deteriorates the measurement results (Section 2.3.1).

- The value of the DM output signal is inaccurate if $V_{\mathrm{sep,DM}}(f) < V_{\mathrm{sep,CM}}(f)\,CMRR/DMTR$ applies, i.e. in presence of a comparably high CM input signal. The value of the CM output signal is inaccurate if $V_{\mathrm{sep,DM}}(f) < V_{\mathrm{sep,CM}}(f)\,CMRR/DMTR$ applies, i.e. in presence of a comparably high DM input signal (Section 2.3.2).

5 Conclusion

Two contributions to the practical measurement of CM and DM components of conducted EMI are detailed. First, the implications of the impedance criterion given with (3) on the measurement errors are investigated. Analytical results obtained for a simplified model are verified by means of a more detailed model of the considered measurement set-up and experimental results. According to the obtained results, only a gain error is expected with the considered measurement configuration, which can be removed by initial calibration. Second, an active CM/DM separator is detailed, which features straightforward realization and competitive separation capability, $DMTR/CMRR > 51\,\mathrm{dB}$ and $CMTR/DMRR > 47\,\mathrm{dB}$ for frequencies up to 10 MHz. A good matching of EMI spectra measured with passive and active separators is presented.

References

[1] IEC 61000-3-2: Electromagnetic compatibility (EMC) – Part 3 Limits, Section 2: Limits for harmonic current emissions (equipment input current 16 A per phase), 2005.

[2] IEC 61000-6-3: Electromagnetic compatibility (EMC) – Part 6 Generic standards, Section 3: Emission standard for residential, commercial and light-industrial environments, 2006.

[3] I. Kovacevic, F. Krismer, S. Schroth, and J. W. Kolar: "Practical characterization of EMI filters replacing CISPR 17 approximate worst case measurements," *Proc. of the IEEE 14th COMPEL 2013*, 10 pp., June 2013.

[4] IEC/CISPR 16-1-2 Specification for radio disturbance and immunity measuring apparatus and methods – Part 1: Radio disturbance and immunity measuring apparatus, Section 2: Ancillary equipment – Conducted disturbances, 2003.

[5] C. Paul and K. B Hardin, "Diagnosis and reduction of conducted noise emmisions," *IEEE Transaction on Electromagnetic Compatibility*, vol. 30, no. 4, pp. 553–560, Nov. 1988.

[6] K.Y. See, "Network for conducted EMI diagnosis," *Electronic Letters*, vol. 35, no. 17, pp. 1446–1447, Aug. 1999.

[7] M. J. Nave, "A novel differential mode rejection network for conducted emissions diagnostics," *IEEE National Symposium on Electromagnetic Compatibility 1989*, pp. 223–227, May 1989.

[8] T. Guo, D.Y. Chen, and F.C. Lee, "Separation of the common-mode- and differential-mode-conducted EMI noise," *IEEE Transaction on Power Electronics*, vol. 11, no. 3, pp. 480–488, May 1996.

[9] A. Nagel and R. W. De Doncker, "Separating common mode and differential mode noise in EMI measurements," *Proc. of the 8th EPE 1999*, 8 pp., Sept. 1999.

[10] S. Wang, F. C. Lee, and W. G. Odendaal, "Characterization, evaluation, and design of noise separator for conducted EMI noise diagnosis," *IEEE Transaction on Power Electronics*, vol. 20, no. 4, pp. 974–982, July 2005.

[11] T. von Rauner, "A measurement system for evaluatiom of the coupling modes and mechanisms of conductive noise," Master's thesis, Electrical and Communications Engineering, Helsinki University of Technology, June 1999.

[12] P.-S. Chen, "Software-based separation of conductive EMI signals," *Proc. of the IEEE 10th IAS 2006*, vol. 3, pp. 1209–1214, Oct. 2006.

[13] J. Kelin, W. Jingmei, W. Chang, and B. Chuang, "A new method for conducted EMI noise diagnosis," *Proc. of the IEEE 8th ICEMI 2007*, pp. 4-59–4-63, Aug. 2007.

[14] Y.-K. Lo, H.-J. Chiu, T.-H. Song, M.-P. Chen, and T.-S. Luor, "A software-based CM and DM measurement system for the conducted EMI," *Proc. of the IEEE 25th IECON 1999*, vol. 1, pp. 253–255, Nov./Dec. 1999.

[15] J. Stahl, D. Kuebrich, and T. Duerbaum, "Modification and characterization of a standard LISN for effective EMI noise separation," *Proc. of the IEEE 12th ICEAA 2010*, pp. 39–42, Sept. 2010.

[16] K. S. Kostov, H.-P. Nee, M. Priecinsky, "The input impedance of common mode and differential mode noise separators," *Proc. of the IEEE 5th ECCE 2013*, pp. 1688–1695, Sept. 2013.